# TIME-FREQUENCY ANALYSIS OF SCATTERING RESPONSES FROM A DIELECTRIC SPHERE

Masahiko NISHIMOTO and Hiroyoshi IKUNO
Department of Electrical and Computer Engineering, Kumamoto University
Kurokami 2-39-1, Kumamoto 860-8555, Japan
E-mail: nisimoto@eecs.kumamoto-u.ac.jp

## 1. INTRODUCTION

In electromagnetic wave scattering by radar targets, several scattering mechanisms contribute to the scattering responses. Although these mechanisms have usually been investigated in either the time or frequency domain, it is not so easy to extract them from the complicated scattering data. In order to investigate them, the joint time-frequency analysis is available and effective. In the time-frequency analysis, the local time and frequency contents of the scattering data are extracted and much better insights can be obtained into the scattering mechanisms. The well-known tools for time-frequency analysis are the short-time Fourier transform (STFT)[1][2], the Wigner-Ville distribution (WVD)[1], and the more recently introduced wavelet transform (WT)[3][4]. Especially, the WT seems to be more useful for its multi-resolution characteristics than others.

In this paper, we analyze the scattering responses from a dielectric sphere in the time-frequency domain by using the WT, and investigated the scattering mechanisms. In the analysis, we use two types of wavelet transforms: one is applied to time responses, and the other to frequency responses. The advantage of the use of these two types of WTs is that the different multiresolution characteristics are available and the information that are not apparent in time or frequency analysis can be extracted from the responses. By investigating the resulting time-frequency displays, we can clearly identify and resolve the scattering mechanisms including reflection, refraction, creeping, and resonances.

## 2. WAVELET TRANSFORM

In the field of signal processing, the WT is usually applied to time-domain data. However, the WT is also applicable to frequency domain data [3]. Since these two types of WTs have different multiresolution characteristics, it is convenient to use both WTs in extracting the target information from scattering data.

### 2-1. Wavelet Transform of Time Domain Data

The continuous WT of time domain data $f(t)$ is defined as follows [5]:

$$W_t(a, b) = \frac{1}{\sqrt{a}} \int_{-\infty}^{\infty} f(t)\, \psi^*\left(\frac{t-b}{a}\right) dt \tag{1}$$

where $\psi(t) \in L^2(\mathbf{R})$ is the prototype wavelet that is called "mother wavelet", and it satisfies an additional "admissibility condition" in wavelet theory [5]. Equation (1) indicates that $W_t(a, b)$ is the integral transform with kernel $\psi((t-b)/a)$ that is the translated and shifted mother wavelet. Physically, the scale parameter $a$ and shift parameter $b$ correspond to the reciprocal of frequency $(1/\omega)$ and time $(t)$, respectively. As the mother wavelet, we consider the Gaussian wavelet given by

$$\psi(t) = \frac{1}{\sqrt{2\pi}\,\sigma_t} \exp\left(-\frac{t^2}{2\sigma_t^2}\right) \cdot \exp(-j\omega_0 t) \tag{2}$$

where $\sigma_t$ and $\omega_0$ are constants that determine the width and the center frequency of the wavelet, respectively. Substituting Eq.(2) into Eq.(1) and applying the Fourier transform, $W_t$ can be rewritten as follows:

$$W_t(T,\Omega) = \sqrt{\frac{\Omega}{2\pi\sigma_t^2}} \int_{-\infty}^{\infty} f(t) \exp\left[-\frac{\Omega^2}{2\sigma_t^2\omega_0^2}(t-T)^2\right] \cdot \exp\left[j\Omega(t-T)\right] dt$$

$$= \frac{1}{2\pi}\sqrt{\frac{\omega_0}{\Omega}} \int_{-\infty}^{\infty} F(\omega) \exp\left[-\frac{\omega_0^2\sigma_t^2}{2}\left(\frac{\omega}{\Omega}+1\right)^2\right] \cdot \exp(j\omega T)\, d\omega \qquad (3)$$

where $F(\omega)$, which is the Fourier transform of $f(t)$, is the frequency response data. In the above expression, we rewrite the parameters $a$ and $b$ as $\omega_0/a = \Omega$ and $b = T$, respectively, because these parameters correspond to the reciprocal of frequency and time as mentioned before. Eq. (3) indicates that $W_t$ is expressed by the window Fourier transform of frequency domain data $F(\omega)$ with variable width Gaussian window function which slides along $\omega$-axis and extracts local information of the data. Since the width of the window changes with frequency $\Omega$, $W_t$ has fine time resolution in high frequency and fine frequency resolution in low frequency. This multi-resolution characteristic is suitable for detecting rapidly changing signal components along the time axis.

### 2-2. Wavelet Transform of Frequency Domain Data

The continuous WT of frequency-domain data $F(\omega)$ is defined as follows:

$$W_f(a,b) = \frac{1}{\sqrt{a}} \int_{-\infty}^{\infty} F(\omega)\, \Psi^*\left(\frac{\omega-b}{a}\right) d\omega \qquad (4)$$

where $\Psi(\omega) \in L^2(\mathbf{R})$ is the mother wavelet that satisfies the admissibility condition. Similar to the WT of time domain data, we choose the Gaussian wavelet as the mother wavelet:

$$\Psi(\omega) = \frac{1}{\sqrt{2\pi}\,\sigma_f} \exp\left(-\frac{\omega^2}{2\sigma_f^2}\right) \cdot \exp(-j\omega t_0) \qquad (5)$$

where $\sigma_f$ and $t_0$ are constants that related to the time-frequency resolution and the center of the wavelet, respectively. By using the above mother wavelet, Eq.(4) is rewritten as follows:

$$W_f(T,\Omega) = \sqrt{\frac{T}{2\pi\sigma_f^2 t_0}} \int_{-\infty}^{\infty} F(\omega) \exp\left[-\frac{T^2}{2\sigma_f^2 t_0^2}(\omega-\Omega)^2\right] \cdot \exp(-j(\omega-\Omega)T) d\omega$$

$$= \frac{1}{\sqrt{T}} \int_{-\infty}^{\infty} f(t) \exp\left[-\frac{\sigma_f^2 t_0^2}{2}\left(\frac{t}{T}-1\right)^2\right] \cdot \exp(-j\Omega t) dt \qquad (6)$$

where we rewrite the parameters $a$ and $b$ as $t_0 / a = T$ and $b = \Omega$, respectively. This expression indicates that $W_f$ is obtained by the window Fourier transform of time domain data $f(t)$ with variable width Gaussian window. Since the width of the window changes with time $T$, $W_f$ has fine time resolution in the early time and fine frequency resolution in the late time. This multi-resolution characteristic is suitable for separating the multi-scale (multi-frequency) signal components along the frequency axis.

## 3. NUMERICAL RESULTS AND DISCUSSIONS

By using $W_t$ and $W_f$, we analyze the pulse responses scattered from a dielectric sphere of radius $a$, and investigate the scattering mechanisms included in the scattering data. As the incident pulse, we choose once differentiated Gaussian pulse. The time axis is normalized by transit time of the pulse for radius $a$ and defined by $\tau = t/(a/c_0)$ where $c_0$ is the light velocity in free space. In order to get the scattering data, we use the well known rigorous solution for the scattering by a dielectric sphere in frequency domain.

Figure 1 shows the gray scale representations of $W_t(T, \Omega)$ of backscattering data from a dielectric sphere with refractive index $N = 3$. Along the time and frequency axes, the time-domain data $f(\tau)$ and its spectrum $F(ka)$ are also plotted. In this figure, we can observe several vertical lines whose widths become narrow in high frequency region. They correspond to the responses of different scattering mechanisms such as specular reflection (SR), $m$-times internal reflection ($IR_m$), creeping (C), and combination of internal reflection and creeping ($IRC_m$). The ray paths obtained by the ray tracing are

illustrated in Fig.2, and the delay times of them calculated by the ray theory are also shown in Table 1. The delay time of each response in Fig.1 agrees well with the calculated value in Table 1. On the other hand, the gray scale representations of $W_f(T, \Omega)$ of backscattering data are shown in Fig.3. In the late time, we can observe many horizontal lines that correspond to the natural frequencies of the dielectric sphere. Table 2 shows the comparison of the real part of the natural frequencies extracted by the present analysis (the peak values of each horizontal line in Fig.3) with the corresponding exact ones obtained by solving characteristic equations. Since a dielectric sphere has a lot of natural frequencies near the real axis, it is difficult to extract and resolve them accurately. However, extracted values agree well with the real part of some natural frequencies. From these results, we can confirm that the scattering mechanisms included in the backscattering data are clearly identified and resolved, and some of the natural frequencies are extracted by the wavelet analysis.

## 4. CONCLUSIONS

The responses scattered from a dielectric sphere have been analyzed in the time-frequency domain by using two types of WTs, and have investigated the scattering mechanisms. From the resulting time-frequency displays, various scattering mechanisms have been identified and resolved, and the natural frequencies have been extracted.

This work was partially supported by the Grant-in-Aid for Scientific Research (grant 11650351) from the Ministry of Education, Science, and Culture, Japan.

## REFERENCES

[1] A.Moghaddar and E.K.Walton, "Time-frequency distribution analysis of scattering from waveguide cavities", IEEE Trans., Antennas & Propagat., vol.41, pp. 677-680, 1993.
[2] L.C.Trintinalia and H.Ling, "Interpretation of Scattering Phenomenology in Slotted Waveguide Structures via Time-Frequency Processing", IEEE Trans., Antennas & Propagat., vol. AP-43, pp. 1253-1261, 1995.
[3] H.Kim and H.Ling,"Wavelet analysis of radar echo from finite-size targets", IEEE Trans., Antennas & Propagat., vol. AP-41, pp. 200-207, 1993.
[4] M. Nishimoto and H. Ikuno, "Time-frequency analysis of scattering data using wavelet transform", Trans. IEICE, vol. E80-C, pp.1440-1447, 1997.
[5] C.K.Chui, "An introduction to wavelets", Academic Press, 1992.

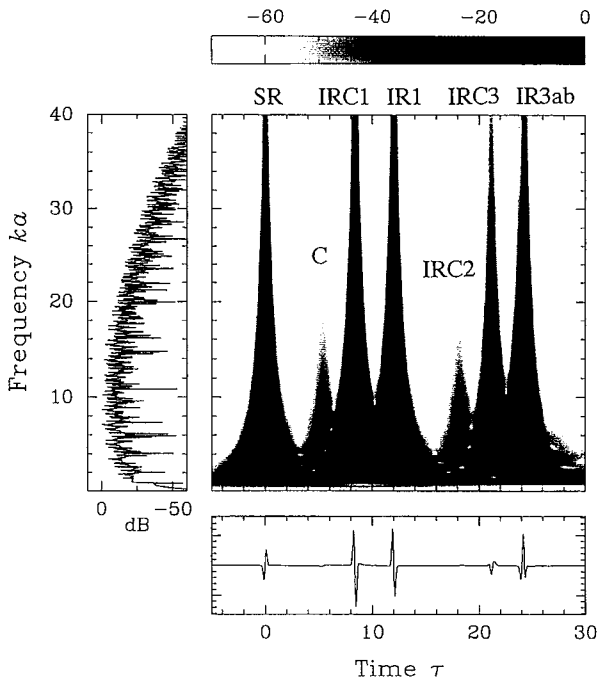


**Fig.1.** Wavelet transform of time domain data $W_f(T, \Omega)$.

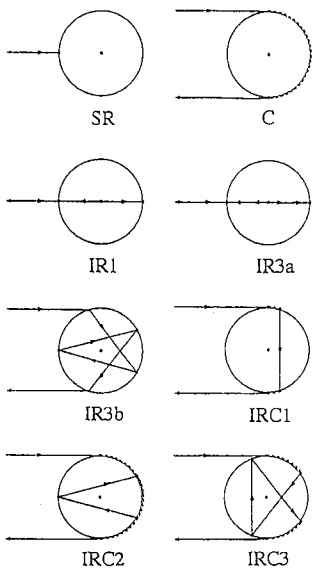


**Fig.2.** Ray paths of scattering mechanisms.

**Table 1.** Delay times calculated by the ray theory.

| Scattering process | SR | C | IR1 | IR3a | IR3b | IRC1 | IRC2 | IRC3 |
|---|---|---|---|---|---|---|---|---|
| Delay time $\tau$ | 0 | 5.14 | 12.00 | 24.00 | 24.21 | 8.34 | 17.81 | 21.01 |

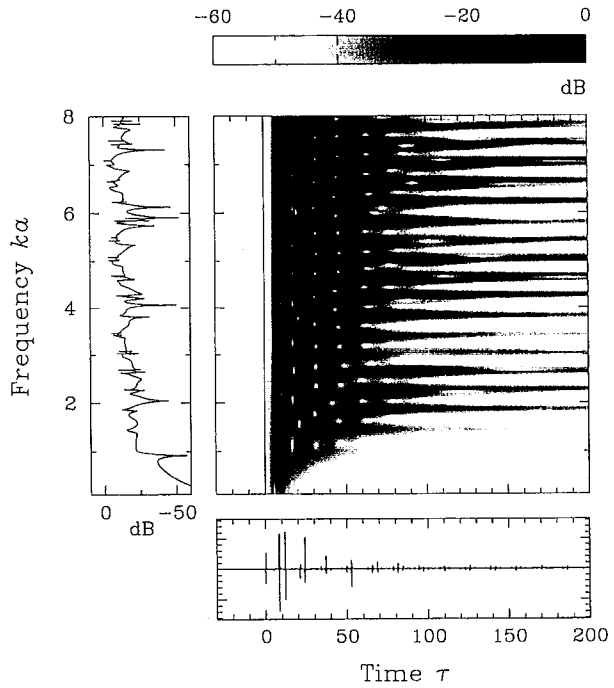


**Fig.3.** Wavelet transform of frequency domain data $W_f(T, \Omega)$.

**Table 2.** Comparison of extracted natural frequencies with exact ones.

| Extracted | Exact | Extracted | Exact | Extracted | Exact |
|---|---|---|---|---|---|
| 1.434 | 1.434 + j 0.027 | 3.419 | 3.397 + j 0.028 | 4.669 | 4.681 + j 0.003 |
| | 1.442 + j 0.179 | | 3.469 + j 0.000 | 5.021 | 5.023 + j 0.005 |
| 1.865 | 1.865 + j 0.011 | | 3.425 + j 0.000 | 5.427 | 5.440 + j 0.002 |
| 2.280 | 2.282 + j 0.004 | 3.832 | 3.833 + j 0.014 | 5.528 | 5.569 + j 0.079 |
| 2.617 | 2.568+ j 0.135 | | 3.852 + j 0.000 | | 5.502 + j 0.000 |
| | 2.624 + j 0.006 | | 3.812 + j 0.000 | 5.800 | 5.807 + j 0.015 |
| 2.705 | 2.686 + j 0.001 | 4.261 | 4.261 + j 0.006 | | 5.849 + j 0.000 |
| 3.034 | 3.081 + j 0.000 | | 4.232 + j 0.000 | 6.239 | 6.266 + j 0.113 |
| | 3.003 + j 0.174 | 4.613 | 4.644 + j 0.102 | | 6.239 + j 0.008 |
| | 3.030 + j 0.002 | | 4.594 + j 0.014 | | 6.228 + j 0.126 |
| | | | 4.573 + j 0.000 | | |